

A quantitative targeted proteomics approach to validate predicted microRNA targets in *C. elegans*

Marko Jovanovic^{1–3,11}, Lukas Reiter^{1–3,10,11}, Paola Picotti⁴, Vinzenz Lange^{4,5,10}, Erica Bogan^{1,2}, Benjamin A Hirschler⁶, Cherie Blenkiron^{7,8,10}, Nicolas J Lehrbach^{7,8}, Xavier C Ding⁶, Manuel Weiss^{1–3}, Sabine P Schrimp^{1,3}, Eric A Miska^{7,8}, Helge Großhans⁶, Ruedi Aebersold^{4,5,9} & Michael O Hengartner^{1,3}

Efficient experimental strategies are needed to validate computationally predicted microRNA (miRNA) target genes. Here we present a large-scale targeted proteomics approach to validate predicted miRNA targets in *Caenorhabditis elegans*. Using selected reaction monitoring (SRM), we quantified 161 proteins of interest in extracts from wild-type and *let-7* mutant worms. We demonstrate by independent experimental downstream analyses such as genetic interaction, as well as polysomal profiling and luciferase assays, that validation by targeted proteomics substantially enriched for biologically relevant *let-7* interactors. For example, we found that the zinc finger protein ZTF-7 was a bona fide *let-7* miRNA target. We also validated predicted miR-58 targets, demonstrating that this approach is adaptable to other miRNAs. We propose that targeted mass spectrometry can be applied generally to validate candidate lists generated by computational methods or in large-scale experiments, and that the described strategy should be readily adaptable to other organisms.

MicroRNA (miRNAs) are short noncoding RNAs that bind to target mRNAs and negatively regulate gene expression. miRNAs are important in many developmental and disease-related processes¹. A full understanding of miRNA function requires knowledge of their target mRNAs. In recent years much progress has been made experimentally and computationally to identify miRNA targets. One of the most widely used approaches to identify potential miRNA targets is to apply different target prediction algorithms¹. However, the many algorithms available predict target sets with only limited overlap and cumulatively identify several hundred potential target mRNAs per miRNA. In addition, large-scale experiments undertaken to identify target mRNAs, such as studies based on mRNA profiling, pulldown of target mRNAs and to a certain extent based on genetics, also identified many potential miRNA targets^{2,3}. Recent publications have clearly

shown that using multiple independent experimental approaches greatly improves the reliability of the results obtained^{4,5}, but large-scale experiments are often cumbersome and time intensive. Therefore we aimed to establish a targeted quantification method to rapidly validate large numbers of potential miRNA targets.

We reasoned that such a method should measure the most relevant output of gene expression, namely miRNA-dependent changes in protein amounts from potential target genes. Moreover, to be worthwhile, the method should be easy to use, fast, sensitive, reproducible, quantitative and scalable, as several hundred proteins have to be tested for each miRNA. A technique that promises to fulfill most of those criteria is proteomics. Indeed several groups have shown that shotgun proteomics can be used to screen for miRNA targets^{4,6}. However, with available shotgun proteomics approaches, the bulk of measurement time is spent on signals not arising from the desired candidate proteins. Moreover, many of the desired proteins might not be assayed owing to the stochastic sampling of the peptide ions that is common to this method. This results in loss of sensitivity and reproducibility to the extent that high-confidence data on candidate targets can only be achieved at a high cost of time and labor. In contrast, a targeted proteomics approach such as selected reaction monitoring (SRM)^{7,8} has the potential for fast and reliable protein quantification of candidate genes. By limiting the measurement to the proteins of interest, the sensitivity and the reproducibility of the measurements increase dramatically. SRM assays can be developed by selecting for each candidate protein one or several proteotypic peptides that unambiguously identify a protein of interest and have favorable detection properties by mass spectrometry⁹.

Here we describe the application of SRM and isotope-coded affinity tag (ICAT)¹⁰ quantification to screen potential *let-7* targets in *Caenorhabditis elegans*. Our targeted proteomics approach provided high-confidence quantification data, which we then mined to identify miRNA targets of biological importance. Independent downstream

¹Institute of Molecular Life Sciences, University of Zurich, Zurich, Switzerland. ²Doctorate Program in Molecular Life Sciences Zurich, Zurich, Switzerland. ³Quantitative Model Organism Proteomics, University of Zurich, Zurich, Switzerland. ⁴Institute of Molecular Systems Biology, ETH Zurich, Zurich, Switzerland. ⁵Competence Center for Systems Physiology and Metabolic Diseases, Zurich, Switzerland. ⁶Friedrich Miescher Institute for Biomedical Research, Basel, Switzerland. ⁷Department of Biochemistry, University of Cambridge, Cambridge, UK. ⁸Wellcome Trust/Cancer Research UK Gurdon Institute, University of Cambridge, Cambridge, UK. ⁹Faculty of Science, University of Zurich, Zurich, Switzerland. ¹⁰Present addresses: Biognosys AG, Zurich, Switzerland (L.R.), DKMS Life Science Lab, Dresden, Germany (V.L.) and Department of Molecular Medicine and Pathology, University of Auckland, Auckland, New Zealand (C.B.). ¹¹These authors contributed equally to this work. Correspondence should be addressed to M.O.H. (michael.hengartner@imls.uzh.ch) or R.A. (aebersold@imsb.biol.ethz.ch).

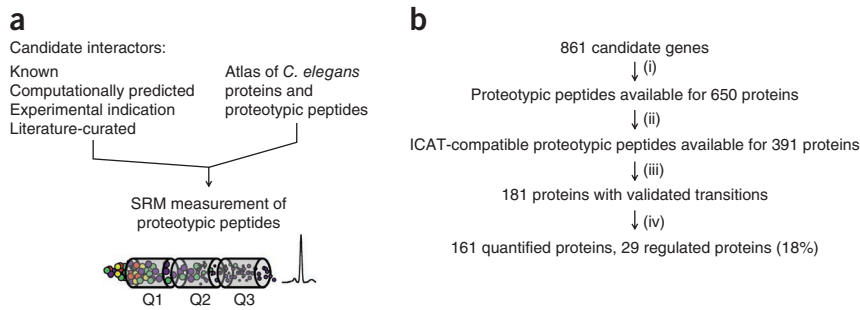


Figure 1 | Strategy and workflow for quantification of potential *C. elegans* *let-7*-interacting genes. **(a)** Proteins of interest were compiled based on predictions, literature search and previous experiments. Proteotypic peptides for these proteins of interest were selected from the *C. elegans* proteome atlas¹⁴. The selected proteotypic peptides were used as probes for reproducible quantification by SRM on a QTrap mass spectrometer operated as a triple quadrupole instrument. **(b)** From the initial 861 genes, 650 proteins had proteotypic peptides in the *C. elegans* proteome atlas (i), of which 391 had cysteine-containing peptides and were quantifiable by ICAT (ii). Validated transitions were derived for 181 proteins (iii), of which 161 could be quantified (iv). Of these, 29 proteins showed significant changes in abundance ($P < 0.01$) between wild type and *let-7(n2853)* mutants (iv).

experiments, including genetic studies, polysomal profiling and luciferase assays, confirmed that the candidate genes classified as regulated by *let-7* based on our protein quantification data were indeed enriched in *let-7* interactors. In addition, we showed that the described method was easily adaptable to another miRNA, miR-58, and quantification strategies other than ICAT, such as metabolic labeling.

RESULTS

SRM-based validation of potential *let-7* target genes

To quantify proteins of interest in a complex whole-worm extract generated from *C. elegans*, we developed a protocol combining ICAT sample labeling and SRM mass spectrometry (**Supplementary Fig. 1** and **Supplementary Results 1**). To test the utility of this protocol, we applied it to screen several hundred potential *let-7* miRNA targets. We focused on *let-7* because it is highly conserved from *C. elegans* to humans¹¹ and is one of the best studied nematode miRNAs¹². We used for our studies the hypomorphic allele *let-7(n2853)*, which contains a point mutation in the mature *let-7* seed sequence that also results in reduced *let-7* expression¹³.

We outline the experimental strategy used to quantify potential *let-7* targets in **Figure 1**. Briefly, we compiled a list of potential *let-7* targets based on predictions from five different algorithms, experimental data (for example, microarray analysis, RNA interference (RNAi) screens and others) and published literature, including known *let-7* target genes. We also included control genes that we knew to be altered in *let-7* mutant worms owing to secondary effects (B.A.H. and H.G., unpublished data) and randomly chosen genes which served as ‘neutral controls’; the final list comprised 861 candidate genes (**Supplementary Table 1** and Online Methods). Proteotypic peptides for 650 proteins of these 861 genes of interest were present in the *C. elegans* proteome atlas^{14,15}, a recently published large *C. elegans* proteomics dataset, in which 8,608 proteins, or about 40% of the proteome, had been identified by shotgun proteomics experiments. For 391 of these, we observed cysteine-containing peptides, a prerequisite for applying ICAT quantification. We experimentally confirmed the presence of 181 (46%) of these 391 proteins by SRM-triggered product ion scan (MS2) measurements in fractionated extracts from synchronized fourth larval stage (L4) worms.

We next compared the abundance of these 181 proteins in synchronized *let-7(n2853)* mutants and wild-type late L4 larvae (when *let-7* expression is highest) in three biological replicates. Most target proteins (139) could be quantified in all three biological replicates, another 15 in two replicates and seven in one replicate, yielding quantification data for a majority of the identified proteins (161 of 181; 89%) and confirming the high reproducibility of this method (**Fig. 2a** and **Supplementary Table 2**). We computed normalized \log_2 ratios (*let-7(n2853)* versus wild type) and corresponding P values for all 161 proteins (**Fig. 2b** and **Supplementary Table 2**).

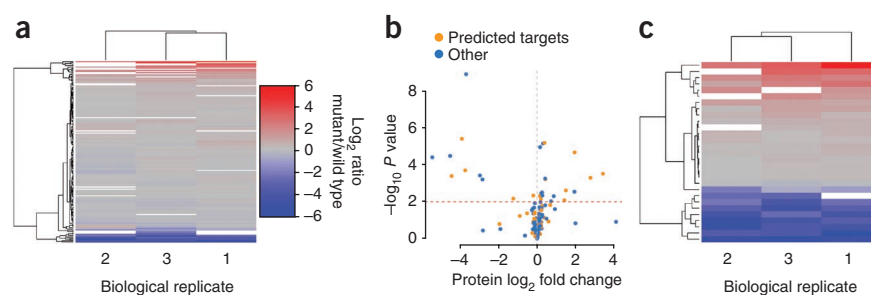
Twenty-nine proteins had a significant difference in expression in *let-7(n2853)* mutants when compared to wild-type worms ($P < 0.01$, one-sample Student’s

t -test; **Fig. 2c** and **Supplementary Table 3**): 10 proteins were downregulated and 19 proteins upregulated in *let-7(n2853)* worms. As expected, the two control genes *vit-2* and *vit-6*, which had greatly reduced mRNA amounts in *let-7(n2853)* mutants (B.A.H. and H.G., unpublished data) were also strongly downregulated in our assay (13-fold and 23-fold, respectively; **Supplementary Table 3**). The upregulated proteins included LET-526 (also known as LSS-4), the only previously reported *let-7* target¹⁶ whose abundance we could measure. Our SRM measurements suggest that the two splice variants of LET-526 responded differently to *let-7*: whereas a peptide specific for the LET-526a splice form showed a strong, 3.1-fold upregulation, a second peptide, matching to a region common to both splice isoforms, displayed only a weak 1.2-fold upregulation in *let-7(n2853)* mutants when compared to wild-type worms (**Supplementary Fig. 2a,b**). We confirmed and validated this splice variant-specific response by polysomal profiling (**Supplementary Fig. 2c** and **Supplementary Results 2**).

Also among the proteins that had significant changes ($P < 0.01$) in expression were 15 of the 66 computationally predicted *let-7* targets, and 9 of the 53 proteins whose mRNA do not contain a predicted *let-7* target site but that have been linked to *let-7* through other experimental approaches or the literature (**Supplementary Table 3**). By contrast, only 2 of the 39 of the randomly picked ‘neutral controls’ had a significant abundance change ($P < 0.01$). The ‘neutral controls’ were the only significantly underrepresented group among the regulated proteins ($P = 0.016$, Fisher’s exact test). This low ‘hit rate’ for these randomly tested proteins confirmed that our initial candidate list was enriched for *let-7* miRNA target genes.

Whether the regulated candidates are primary or secondary targets of *let-7* cannot be determined from the protein ratios. Although the most straightforward explanation for proteins downregulated in *let-7(n2853)* mutants is secondary effects, miRNAs have recently been reported to act as positive regulators under certain conditions¹⁷. A gain of function caused by the point mutation in the seed region of the mature *let-7* miRNA in *let-7(n2853)* mutants, resulting in better binding to a suboptimal seed sequence, also cannot be excluded at this point.

Figure 2 | Identification of proteins regulated by let-7. (a) Heat map and hierarchical clustering of the 161 quantified proteins in three biological replicates. Red and blue indicate up- and downregulated proteins in *let-7(n2853)* mutants, respectively. (b) Volcano plot showing normalized mean \log_2 ratios (vertical gray line indicates no change in expression: \log_2 ratio(*let-7(n2853)*/wild type) = 0) and probability of regulation ($-\log(P$ value)) of the measured proteins. All proteins above the dotted red line ($P = 0.01$) were considered to be significantly regulated ($P < 0.01$). (c) Heat map and hierarchical clustering of the 29 significantly regulated proteins ($P < 0.01$). Color bar as in a.



SRM-based validation enriches for let-7 genetic interactors

let-7(n2853) mutant worms grown at 25 °C die at the adult stage because of vulval bursting. RNAi knockdown of known let-7 miRNA targets has been shown in some cases to rescue this lethality to different extents¹⁶. To determine whether the positive hits in our proteomics screen are indeed enriched in let-7 targets, we knocked down all 29 genes that showed protein changes in *let-7(n2853)* mutants (up- or downregulated) to determine whether they could suppress the *let-7(n2853)* lethal phenotype. Six of the 29 genes knocked down by RNAi caused either larval arrest or lethality, and thus could not be scored for suppression of vulval bursting. For the remaining 23 genes tested, ten reproducibly rescued the lethality to at least 20%, whereas less than 5% of the *let-7(n2853)* worms treated with negative control RNAi survived as adults (Fig. 3a and Supplementary Table 4). As expected, the vast majority (9/10) of the suppressors were genes that were

upregulated in *let-7(n2853)* mutants (and whose overexpression could thus be compensated via RNAi knockdown). As a control, we performed a similar experiment using 29 candidate genes that did not show significant protein changes ($P > 0.1$) in our targeted proteomics assay. Again, five genes either caused early larval arrest or lethality and could not be characterized further. Only three out of the remaining 24 candidates rescued the lethality (Fig. 3b and Supplementary Table 5), demonstrating that the regulated protein set is significantly enriched for genes that genetically interact with let-7 ($P = 0.024$ for all regulated genes, $P = 0.013$ considering only the upregulated genes, Fischer's exact test; Supplementary Fig. 3). We conclude that our targeted proteomics method can indeed be used to enrich for miRNA interaction partners from a list of candidate genes.

Partial correlation between protein and mRNA abundances

In addition to causing translational repression, miRNAs can also lead to degradation of their targets¹. To determine whether the changes in protein levels that we observed could also be captured at the mRNA level, we determined by reverse transcription-quantitative PCR transcript amounts of all 161 proteins as well as of the well established let-7 targets *daf-12* and *lin-41*, in wild-type and *let-7(n2853)* worms (Supplementary Table 6). The amounts of both *daf-12* and *lin-41* mRNA were significantly upregulated in *let-7(n2853)* mutants ($P = 0.006$ and 0.048 , respectively, one-sided one sample Student's *t*-test), as has been reported previously^{18,19}. Whereas some proteins had very good correlation between changes in amounts of mRNA and protein, others, including the known let-7 target *let-526*, showed substantial changes in protein amounts but no strong changes in mRNA amounts (Fig. 4a). As our method cannot distinguish primary from secondary targets, we do not know at this point whether the proteins that showed strong protein changes but no mRNA changes are primary let-7 targets.

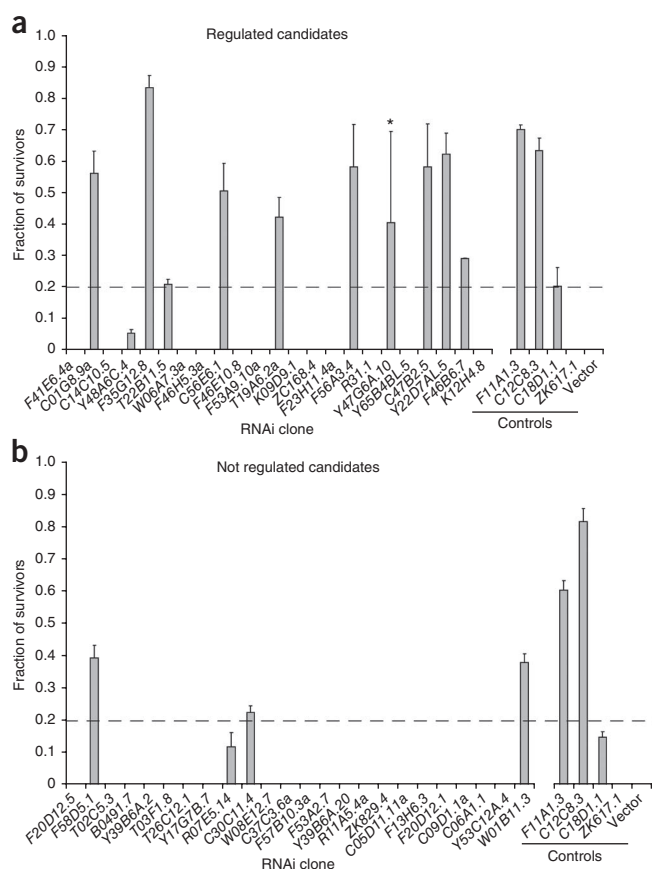


Figure 3 | Genes displaying protein changes in *let-7(n2853)* mutants are enriched in let-7 suppressors. (a) RNAi knockdown of 23 genes that showed significant protein changes ($P < 0.01$) and 5 control genes. The controls included two negative controls (vector and *ZK617.1* (*unc-22*) RNAi) and three positive controls (*F11A1.3* (*daf-12*), *C12C8.3* (*lin-41*) and *C18D1.1* (*die-1*) RNAi). Only survival rates above 5% are shown. (b) As a control, 24 candidates that did not show a significant protein amount change ($P > 0.1$) in the *let-7(n2853)* mutant worms in our targeted proteomics assay were tested as in a, including the same positive and negative controls. Error bars, s.e.m. ($n = 3$). *, suppression in two out of three replicate experiments. The candidate was regarded as positive as the average survival rate over all three replicates was above the threshold. Dashed lines indicate survival rate of 20%.

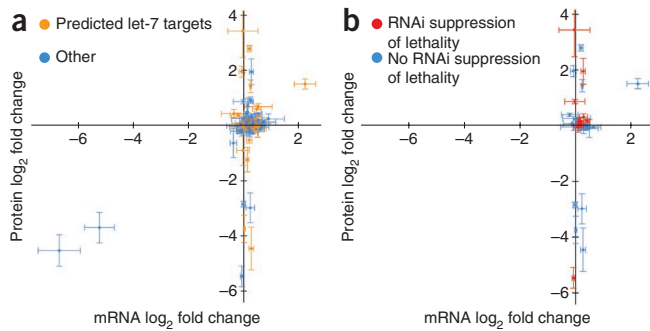


Figure 4 | Comparison of let-7-dependent changes in protein and transcript amounts of candidate let-7 miRNA targets. (a,b) Log₂ fold changes at the mRNA (x axis) and protein (y axis) level between *let-7(n2853)* mutant and wild-type worms for all 161 proteins measured (a) and the subgroup of the 47 candidates scored by RNAi (b). Error bars, s.e.m. ($n = 3$).

We next focused our attention on the 47 genes that we previously tested for suppression of *let-7(n2853)* lethality (see above). Whereas many of the 13 RNAi suppressors showed large changes in protein amounts in *let-7(n2853)* mutants, their mRNA levels varied only weakly, if at all (Fig. 4b). We conclude that many of the protein changes we detected in our targeted proteomics approach are not recapitulated on the mRNA level, and that although mRNA profiling can identify many primary targets^{4,5}, it would not detect several of the biologically important candidates revealed by protein quantification.

zft-7 is a bona fide let-7 target gene

One of the most interesting candidates from our RNAi screen was *zft-7* (F46B6.7), a gene belonging to the zinc finger transcription factor family, as knockdown of this gene not only suppressed lethality (Fig. 3 and Supplementary Table 4) but also the sterility observed in *let-7(n2853)* mutants at 25 °C (data not shown). Of the genes that we tested, only the two positive controls *daf-12* and *lin-41* could also suppress both defects. Consistent with our RNAi results, lethality was strongly reduced in *zft-7(tm600);let-7(n2853)* double mutant worms when compared to the *let-7(n2853)* single mutants (Fig. 5a).

Our SRM measurements had indicated that ZTF-7 protein levels are elevated by ~10% in *let-7(n2853)* mutants when compared to wild-type worms. Although this increase is admittedly mild, it was reproducible across all three biological replicates and significant ($P = 0.005$, one-sample Student's *t*-test; Supplementary Table 3).

As *zft-7* is predicted to contain a conserved perfect seed complementary let-7 binding site in its 3' untranslated region (UTR)^{20,21} we next tested whether the *zft-7* 3' UTR could confer let-7-dependent regulation of a reporter transcript. It has been reported that certain *C. elegans* 3' UTRs can elicit an miRNA-dependent response in human cell lines²². As the sequence of the mature let-7 miRNA is identical in worms and in humans¹¹, we could rapidly test the effect of both overexpression and depletion of human let-7a miRNA in HeLa cells, which we transfected with a dual luciferase plasmid in which the *zft-7* 3' UTR was cloned directly downstream of the firefly luciferase gene (*luciferase::zft-7* 3' UTR). Indeed, we observed a strong response of the *luciferase::zft-7* 3' UTR reporter to both human let-7a up- and downregulation (Fig. 5b).

Taken together, our proteomic, genetic and reporter assays strongly suggest that *zft-7* is a bona fide let-7 miRNA target. Moreover, *zft-7* also has been identified recently as a potential let-7 target by a new approach²³, providing independent support for our claim. Additionally that method also allowed mapping of the binding site, which overlapped perfectly with the predicted conserved seed site. Further work will be required to understand the function of ZTF-7 in *C. elegans* development.

A streamlined pipeline for miRNA target validation

To test the generality of our targeted proteomics approach, we performed a second experiment to validate predicted targets of miR-58. *mir-58* is of particular interest as it is part of an miRNA gene family. Whereas the single *mir-58* family mutants show no obvious defect, the whole-family knockout is severely sick²⁴. Therefore, it was unclear whether predicted miR-58 targets would show substantial changes in single mutants.

In this second experiment we introduced several technical improvements. First, to target the full peptide repertoire of *C. elegans* and not just cysteine-containing peptides, we used metabolically heavy isotope-labeled worms²⁵ as a quantification standard. Second, we used crude chemically synthesized peptides to establish and optimize the SRM assays²⁶. Third, we applied a newly developed algorithm that automatically assigns peak groups to their corresponding peptides and controls the false discovery rate (FDR) of those assignments (L.R., O. Rinner, P.P., R. Hüttenhain, M. Beck, M. Brusniak *et al.*, unpublished data).

The TargetScan^{20,21} program predicted 118 miR-58 target genes in *C. elegans*. To validate this candidate list, we used crude synthetic peptides for all 118 proteins to develop and optimize SRM assays. We also developed SRM assays for 42 'neutral control' genes that we randomly selected from 5,000 genes that were well expressed in L4 hermaphrodites (data not shown). We next measured the relative amounts of as many of these proteins as possible directly in complex, unfractionated extracts derived from staged L4 wild-type and *mir-58(n4640)* mutant worms. Applying a 5% FDR cutoff for the correct peak assignment, we quantified 27 of the 118 predicted targets and 24 of the 42 randomly chosen proteins in at least one replicate pair

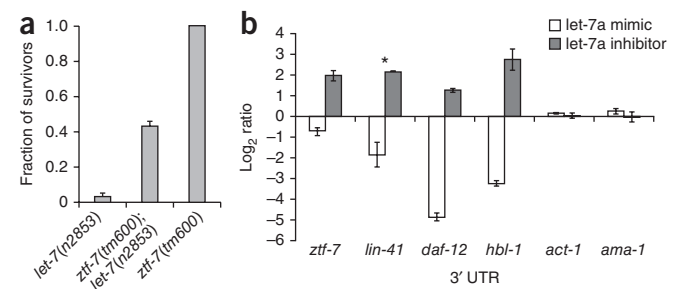


Figure 5 | *zft-7* (F46B6.7) is a bona fide let-7 target gene. (a) Analysis of worm survival 12 h after L4 in the indicated mutants. Error bars, s.e.m. ($n = 4$). (b) Relative luciferase activities for reporter constructs containing the indicated 3'-UTR sequences. The let-7a readouts (mimics and inhibitors) were normalized to their respective oligo controls. The 3' UTRs of the known targets *C12C8.3* (*lin-41*), *F11A1.3* (*daf-12*) and *F13D11.2* (*hbl-1*) were positive controls, and the 3' UTRs of *F36A4.7* (*ama-1*) and *T04C12.6* (*act-1*) were negative controls¹⁶. Transfections were performed in triplicate for all candidates but *lin-41* (*), which was only transfected in duplicate. Error bars, s.e.m.

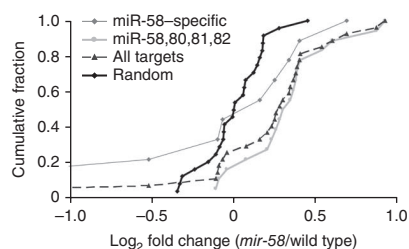


Figure 6 | Predicted miR-58 targets are significantly upregulated in *mir-58*(n4640) mutants. Cumulative fraction plots of the protein response of all 27 measured, predicted miR-58 targets (predicted by TargetScan^{20,21}) as well as of the two subgroups of only miR-58-specific targets (9 of 27) and targets common to all miR-58 family members (miR-58, -80, -81 and -82; 18 of 27) and of a random gene group upon *mir-58* knockout. Data are shown as log₂ ratios (*mir-58*(n4640) to wild type). Both the overall group as well as the whole family subgroup were significantly upregulated in *mir-58*(n4640) mutant worms when compared to the proteins that we randomly chose ($P < 10^{-3}$, Kolmogorov-Smirnov test).

(Supplementary Table 7). Predicted miR-58 targets were, as a group, significantly more likely to be upregulated in *mir-58*(n4640) mutant worms when compared to the randomly chosen control group (Fig. 6; $P < 10^{-3}$, Kolmogorov-Smirnov test). Consistent with this observation, we found that 4 of 27 predicted targets, compared to 1 of 24 control proteins, were significantly upregulated in *mir-58*(n4640) mutant worms ($P < 0.05$, one-sided, one-sample Student's *t*-test; Supplementary Table 7).

miR-58 is a member of a highly abundant miRNA family that also includes miR-80, miR-81, miR-82 and the recently discovered miR-1834 (ref. 24). As expected, TargetScan predicts largely overlapping sets of targets for the various miR-58 family members. Thus, the miR-58 family might show substantial redundancy, as loss of a single miRNA might be compensated by the other family members. Consistent with this hypothesis, single *mir-58* family mutants are all overtly wild type, whereas the *mir-58,80,81,82* quadruple mutant is severely sick. Despite this redundancy at the organismal level, we found that targets predicted to be bound by all miR-58 family members (18 of 27) still showed a significant increase in abundance in *mir-58*(n4640) mutants (Fig. 6; $P < 10^{-3}$, Kolmogorov-Smirnov test). Analysis of protein amounts in the family knockout will be necessary to determine the exact extent of compensation that occurs, if any, in this miRNA family.

DISCUSSION

Our results demonstrate that a targeted proteomics approach can be used to find biologically relevant candidate miRNA targets. First, our method measures changes in protein levels, arguably the most relevant assay for miRNA activity. Second, our approach allows for quantification of several hundred proteins and thus has a much higher throughput than traditional protein quantification methods such as immunoblotting. Additionally, it is much faster and cheaper to develop suitable mass spectrometric assays than immunoassays²⁶. Moreover, once an SRM assay is established for a protein, it becomes universally useful and exportable^{8,27}. Thus, others can readily use the SRM assays we established for the 312 *C. elegans* proteins that we measured (Supplementary Tables 8 and 9). Third, because it focuses on highly responsive peptides, our SRM-based approach is highly sensitive and reproducible.

Indeed, we reproducibly measured changes as small as 10% in total protein abundance, as exemplified with ZTF-7. This high accuracy is particularly important in the analysis of potential miRNA targets, as miRNAs have been shown to mostly induce small changes in target gene expression^{4,6}.

Despite the clear value of our targeted proteomics approach, several challenges remain. First, although we achieved high sensitivity, we still did not quantify a substantial fraction of the proteins in our target list. Technical improvements, such as using a combination of chemically synthesized peptides and sample fractionation, could potentially boost the sensitivity by an order of magnitude, as has previously been shown in yeast⁷. Second, the targeted proteomics approach cannot be used to distinguish primary from secondary targets. Additional experiments will thus invariably be necessary to establish which hits are direct targets, as we did for *ztf-7*.

We also stress that the applicability of our targeted proteomics method to whole organs or whole animals is particularly challenging, as the miRNA of interest might be of low abundance or have a highly restricted expression pattern. We therefore conclude that our method will function best in situations in which sufficient material can readily be obtained and the sample is homogenous (for example, cell lines; Supplementary Discussion).

The targeted proteomics approach described here should be considered complementary to the shotgun proteomics approaches recently reported to identify miRNA targets^{4,6}. Whereas shotgun proteomics should be regarded as one of several discovery tools that can be used to find potential new miRNA target candidates, a targeted proteomics approach should be perceived as a validation and hypothesis-driven tool with high sensitivity, reproducibility and accuracy.

Although here we validated miRNA targets in *C. elegans*, the targeted proteomics method is broadly applicable and could be readily adapted to study other organisms and other biological questions. Many quantification methods are available²⁸, suitable for nearly every extract composition. In addition, public proteomics databases for many organisms are available, from which experimentally identified proteins and their corresponding proteotypic peptides can be easily mined^{29,30}. Even for organisms for which such proteomics data are not readily accessible, sophisticated proteotypic peptide prediction algorithms⁹ can be used to target the right peptides. Thus, the targeted proteomics approach described here can be applied generally to measure protein abundances of candidate lists generated by computational methods or in large-scale experiments.

METHODS

Methods and any associated references are available in the online version of the paper at <http://www.nature.com/naturemethods/>.

Note: Supplementary information is available on the Nature Methods website.

ACKNOWLEDGMENTS

We thank R.F. Ketting (Hubrecht Institute, Utrecht) and B.B. Tops (Utrecht University, Utrecht) for providing the metabolically labeled *C. elegans* sample, A. Stark (Research Institute of Molecular Pathology, Vienna) for sharing miRNA target predictions for *C. elegans*, M. Moser for the assistance with the reverse transcription-quantitative PCR assays, B. Roschitzky and B. Gerrits for technical support, H. Rehrauer for statistical support, R. Schlapbach for access to the Functional Genomics Center Zurich, members of the Hengartner, Aebersold, Grosshans and Miska laboratories and E. Brunner and the whole Quantitative Model Organism Proteomics team for insightful discussion and comments on the

manuscript. This work was funded in part by the University of Zurich Research Priority Program in Systems Biology/Functional Genomics, the Swiss National Science Foundation, the Gerbert R uf Foundation, the Swiss initiative for systems biology, SystemsX, the Ernst Hadorn Foundation and the ETH Zurich. R.A. was supported by the European Research Council grant ERC-2008-AdG 233226. M.J. and L.R. were supported by a grant from the Research Foundation of the University of Zurich. M.J. was also supported by a fellowship from the Roche Research Foundation. P.P. was supported by the Marie Curie Intra-European fellowship. V.L. was supported by a grant from F. Hoffmann-La Roche Ltd. to the Competence Center for Systems Physiology and Metabolic Diseases. H.G. was supported by the Swiss National Research Foundation, the Novartis Research Foundation and by an ERC Starting Investigator grant (miRTurn). X.C.D. was supported by a Boehringer Ingelheim Funds PhD Student fellowship. C.B., N.J.L. and E.A.M. were supported by a Cancer Research UK Programme grant to E.A.M.

AUTHOR CONTRIBUTIONS

M.J., L.R., M.O.H. and R.A. designed the experiments and wrote the paper. L.R. and M.J. did the majority of the data analysis. M.J. did the majority of the experiments. P.P. and V.L. contributed to and supervised the SRM experiments. E.B. contributed to the RNAi and reverse transcription-quantitative PCR experiments. B.A.H. and X.C.D. performed the polysomal profiling experiments. C.B. and N.J.L. contributed to the reporter assays. S.P.S. and M.W. provided the *C. elegans* proteome atlas. H.G. and E.A.M. provided critical input on the manuscript, contributed to the experimental design and the data analysis. M.O.H. and R.A. supervised the project.

COMPETING FINANCIAL INTERESTS

The authors declare no competing financial interests.

Published online at <http://www.nature.com/naturemethods/>.

Reprints and permissions information is available online at <http://npg.nature.com/reprintsandpermissions/>.

- Bartel, D.P. MicroRNAs: target recognition and regulatory functions. *Cell* **136**, 215–233 (2009).
- Lai, E.C. miRNAs: whys and wherefores of miRNA-mediated regulation. *Curr. Biol.* **15**, R458–R460 (2005).
- Ørom, U.A. & Lund, A.H. Experimental identification of microRNA targets. *Gene* **451**, 1–5 (2010).
- Baek, D. *et al.* The impact of microRNAs on protein output. *Nature* **455**, 64–71 (2008).
- Hendrickson, D.G. *et al.* Concordant regulation of translation and mRNA abundance for hundreds of targets of a human microRNA. *PLoS Biol.* **7**, e1000238 (2009).
- Selbach, M. *et al.* Widespread changes in protein synthesis induced by microRNAs. *Nature* **455**, 58–63 (2008).
- Picotti, P., Bodenmiller, B., Mueller, L.N., Domon, B. & Aebersold, R. Full dynamic range proteome analysis of *S. cerevisiae* by targeted proteomics. *Cell* **138**, 795–806 (2009).
- Picotti, P. *et al.* A database of mass spectrometric assays for the yeast proteome. *Nat. Methods* **5**, 913–914 (2008).
- Mallick, P. *et al.* Computational prediction of proteotypic peptides for quantitative proteomics. *Nat. Biotechnol.* **25**, 125–131 (2007).
- Gygi, S.P. *et al.* Quantitative analysis of complex protein mixtures using isotope-coded affinity tags. *Nat. Biotechnol.* **17**, 994–999 (1999).
- Pasquinelli, A.E. *et al.* Conservation of the sequence and temporal expression of let-7 heterochronic regulatory RNA. *Nature* **408**, 86–89 (2000).
- Bussing, I., Slack, F. & Großhans, H. let-7 microRNAs in development, stem cells and cancer. *Trends Mol. Med.* **14**, 400–409 (2008).
- Reinhart, B.J. *et al.* The 21-nucleotide let-7 RNA regulates developmental timing in *Caenorhabditis elegans*. *Nature* **403**, 901–906 (2000).
- Schrimpf, S.P. *et al.* Comparative functional analysis of the *Caenorhabditis elegans* and *Drosophila melanogaster* proteomes. *PLoS Biol.* **7**, e48 (2009).
- Reiter, L. *et al.* Protein identification false discovery rates for very large proteomics data sets generated by tandem mass spectrometry. *Mol. Cell. Proteomics* **8**, 2405–2417 (2009).
- Großhans, H., Johnson, T., Reinert, K., Gerstein, M. & Slack, F. The temporal patterning microRNA regulates several transcription factors at the larval to adult transition in *C. elegans*. *Dev. Cell* **8**, 321–330 (2005).
- Vasudevan, S., Tong, Y. & Steitz, J.A. Switching from repression to activation: microRNAs can up-regulate translation. *Science* **318**, 1931–1934 (2007).
- Bagga, S. *et al.* Regulation by let-7 and lin-4 miRNAs results in target mRNA degradation. *Cell* **122**, 553–563 (2005).
- Ding, X.C. & Großhans, H. Repression of *C. elegans* microRNA targets at the initiation level of translation requires GW182 proteins. *EMBO J.* **28**, 213–222 (2009).
- Lewis, B.P., Burge, C.B. & Bartel, D.P. Conserved seed pairing, often flanked by adenosines, indicates that thousands of human genes are microRNA targets. *Cell* **120**, 15–20 (2005).
- Ruby, J.G. *et al.* Large-scale sequencing reveals 21U-RNAs and additional microRNAs and endogenous siRNAs in *C. elegans*. *Cell* **127**, 1193–1207 (2006).
- Nottrott, S., Simard, M.J. & Richter, J.D. Human let-7a miRNA blocks protein production on actively translating polyribosomes. *Nat. Struct. Mol. Biol.* **13**, 1108–1114 (2006).
- Andachi, Y. A novel biochemical method to identify target genes of individual microRNAs: Identification of a new *Caenorhabditis elegans* let-7 target. *RNA* **14**, 2440–2451 (2008).
- Alvarez-Saavedra, E. & Horvitz, H.R. Many families of *C. elegans* microRNAs are not essential for development or viability. *Curr. Biol.* **20**, 367–373 (2010).
- Krijgsveld, J. *et al.* Metabolic labeling of *C. elegans* and *D. melanogaster* for quantitative proteomics. *Nat. Biotechnol.* **21**, 927–931 (2003).
- Picotti, P. *et al.* High-throughput generation of selected reaction-monitoring assays for proteins and proteomes. *Nat. Methods* **7**, 43–46 (2010).
- Addona, T.A. *et al.* Multi-site assessment of the precision and reproducibility of multiple reaction monitoring-based measurements of proteins in plasma. *Nat. Biotechnol.* **27**, 633–641 (2009).
- Mueller, L.N., Brusniak, M., Mani, D.R. & Aebersold, R. An assessment of software solutions for the analysis of mass spectrometry based quantitative proteomics data. *J. Proteome Res.* **7**, 51–61 (2008).
- Brunner, E. *et al.* A high-quality catalog of the *Drosophila melanogaster* proteome. *Nat. Biotechnol.* **25**, 576–583 (2007).
- Baerenfaller, K. *et al.* Genome-scale proteomics reveals *Arabidopsis thaliana* gene models and proteome dynamics. *Science* **320**, 938–941 (2008).

ONLINE METHODS

Mutations and strains. All mutants used in this study were derived from the wild-type variety Bristol strain N2. The following mutations were used: LGIII, *unc-119(ed3)* (ref. 31); LGIV, *miR-58(n4640)* (ref. 32); LGV, *ztf-7(tm600)* (<http://www.wormbase.org/>); LGX, *let-7(n2853)* (ref. 13); *ain-1(ku322)* (ref. 33); *alg-1(tm492)*; and transgene, *opIs205* ($P_{eft-3}::TAPtag::alg-1(\text{genomics}+3'UTR);unc-119(+)$). The *alg-1(tm492)* mutant was obtained from the laboratory of S. Mitani (Tokyo Women's Medical University Hospital) and outcrossed four times. The 610-bp deletion was confirmed by PCR amplification.

For the miR-58-related experiments only, the transgenic line carrying *opIs205* was crossed into *alg-1(tm492)* mutant worms to generate the strain WS4303 (*alg-1(tm492);opIs205*), to which we refer as 'wild type'. WS4303 was also crossed into *mir-58(n4640)* worms to generate the strain WS5041 (*mir-58(n4640);alg-1(tm492);opIs205*), to which we refer to as 'mir-58(n4640)'.

Sample preparation for let-7-related experiments. *C. elegans* strains were grown as described previously³⁴ at either 15 °C or 25 °C.

C. elegans wild-type strain N2 (Bristol) and the *let-7(n2853)* mutant strain MT7626 were grown on 9-cm nematode growth medium (NGM) agar plates seeded with a lawn of the *Escherichia coli* strain OP50. N2 and *let-7(n2853)* worms were always grown in parallel (three biological replicates total). Protein extracts were generated from synchronized late L4 larval stage worms (before vulval bursting), which were grown at 25 °C. Worms were collected and washed three times in M9 medium. Generation of the protein extract has been described previously¹⁴. The protein concentrations of the purified extracts were determined by using the Bradford reagent (Sigma-Aldrich). The protein concentrations of N2 and *let-7(n2853)* extracts were adjusted to each other to minimize biases for the subsequent ICAT (Applied Biosystems) labeling¹⁰.

ICAT labeling, tryptic digestion of the samples, and the isolation and clean up of ICAT labeled cysteine-containing peptides were performed as described previously³⁵. N2 extracts were always labeled with the heavy ICAT reagent and *let-7(n2853)* extracts with the light ICAT reagent. A total of 5 mg per sample and replicate was labeled, resulting in ~500 µg of ICAT-labeled peptides. The resulting peptide samples were separated according to the isoelectric point of the peptides by off-gel electrophoresis and then cleaned as previously described⁷. All peptide samples were dried in a vacuum centrifuge, resolubilized in 2% acetonitrile and 0.1% formic acid and frozen at -20 °C until analyzed on the mass spectrometer.

Reverse transcription-quantitative PCR (RT-qPCR). Before protein isolation, a small aliquot of intact worms of each biological replicate (three times N2 wild-type worms and three times *let-7(n2853)* worms; see above) was frozen, and then used for total RNA isolation. Total RNA was isolated using the Nucleo Spin RNA II kit (Macherey-Nagel) according to the manufacturer's instructions. After total RNA isolation, genomic DNA was further digested by DNase I using the Turbo DNA-free kit (Ambion) according to the manufacturer's instructions. Total RNA concentrations were determined with the Nanodrop device

(Thermo Fisher Scientific). RNA reverse transcription was performed using the Transcriptor High Fidelity cDNA Synthesis kit (Roche) with oligo-(dT) primers, according to the manufacturer's recommendations using equal amounts of RNA (4 × 2 µg) for each sample. qPCR reactions were performed in technical duplicate for each of the biological triplicates using MESA Green qPCR Mastermix Plus for SYBR Assay (Eurogentec), according to the manufacturer's recommendations, on an ABI 7900 HT Sequence Detection System coupled to ABI Prism 7900 SDS 2.2 Software (Applied Biosystems). Relative transcript amounts were calculated using the $2^{-\Delta\Delta C_t}$ method³⁶. The following genes were used as internal control genes for normalization: *F11C3.3 (unc-54)*, *T03F1.3 (pgk-1)*, *F43C1.2 (mpk-1)*, *T20B12.2 (tbp-1)* and *F36A4.7 (ama-1)*. Most primer pairs were designed via the Roche Universal Probe Library. All the primer pairs used are listed in **Supplementary Table 10**.

Polysomal profile analysis and subsequent RT-qPCR. The polysomal profile analysis and subsequent RT-qPCR was performed using the same polysomal fractions and protocols as previously described¹⁹. The experiments were performed in triplicate.

We could not develop an RT-qPCR assay specific for *let-526b* only, as there is just a small region (<50 bp) in this splice form that is not present in *let-526a*. Instead we used primers specific for both splice forms. The primers used for *let-526a* specifically were 5'-accacgaccaccatcatc-3' and 5'-cgggcattgtagaagagagc-3'. The primers for both *let-526a* and *let-526b* were 5'-tcgccgagagat tactcgtt-3' and 5'-agaagcgatgcaagagcat-3'.

RNAi experiments. The suppression of *let-7(n2853)* lethality by RNAi knockdown of candidate genes was tested as previously described¹⁶. Briefly, gene knockdown was achieved through RNAi by feeding³⁷⁻⁴⁰. Media supplements were used at the following concentrations: 200 µg ml⁻¹ ampicillin and 2 mM isopropyl-β-D-thiogalactopyranoside (IPTG). All the experiments were performed at 25 °C. About 100-150 synchronized L1 worms were placed on IPTG and AMP NGM agarose plates seeded with 200 µl *E. coli* expressing dsRNA. The worms were scored 72 h later (adult stage) for suppression of lethality. Clones were regarded as positive when at least 20% of the worms were viable as adults. All the clones used were verified by sequencing for their correct insert. All RNAi plasmids used are listed in **Supplementary Table 11**.

Lethality assays for C. elegans mutant strains. All the experiments were performed at 25 °C and in quadruplicate. About 100-150 synchronized L1 worms were placed on NGM agarose plates seeded with 250 µl of OP50 *E. coli* bacteria. The worms were scored 48 h later (12 h after L4) for suppression of lethality. Following strains were tested: MT7626 (*let-7(n2853)*), FX00600 (*ztf-7(tm600)*) and WS5673 (*ztf-7(tm600);let-7(n2853)*). At least 20% of the worms had to be viable in the double-mutant worms (WS5673) to be regarded as a successful suppressor.

Most double-mutant worms (WS5673) were dead 24 h after L4, suggesting more a lethality delay than a true suppression. A developmental delay in WS5673 worms could be excluded as the survivors at the 12 h after L4 time point had fully developed gonads with oocytes and at least 60% of the survivors also had embryos.

Cloning of 3' UTRs from candidate genes. pEM393 is a dual luciferase Gateway (Invitrogen) compatible vector, adapted from the psiCHECK-II vector (Promega). The 3' UTRs of *F46B6.7* (*ztf-7*), *C12C8.3* (*lin-41*), *F11A1.3a* (*daf-12*), *F13D11.2* (*hbl-1*), *F36A4.7* (*ama-1*) and *T04C12.6* (*act-1*) were cloned directly downstream of the firefly luciferase gene. The 3' UTRome *C. elegans* database⁴¹ (<http://www.utrome.org/>) and Wormbase (<http://www.wormbase.org/>) were used to retrieve the sequences for the 3' UTRs of interest. The primers used for PCR and the length of each putative 3' UTR sequence cloned are listed in **Supplementary Table 12**. Gateway cloning was performed according to the manufacturer's instructions (Invitrogen). Briefly, the sequences of interest were amplified using the *attB* adaptor primer PCR protocol to generate PCR clones containing the 3' UTR flanked by respective *attB* sites (*attB1* site at the 5' end and the *attB2* site the 3' end). The PCR product was recombined into pDONR221 by the BP reaction to create the entry clone set (**Supplementary Table 12**). The entry clones were verified by sequencing and then recombined with the destination vector pEM393 to generate the expression clones via the LR reaction (**Supplementary Table 12**). The expression clones were again verified by sequencing and used for the subsequent luciferase assays.

Luciferase assay. The reactions were performed in 96-well plates. miRNA mimics or inhibitors were ordered from Dharmacon. We transfected 150 ng of the dual luciferase expression clone containing the 3' UTR of interest and 10 pmol of either the human *let-7a* mimic, the control mimic (*C. elegans* miR-67), the human *let-7a* inhibitor or the control inhibitor (against *C. elegans* miR-67) into HeLa cells (10,000 cells per reaction) in triplicate. The Dual-Glo Luciferase assay system (Promega) was used 48 h after transfection, according to the manufacturer's instructions. All the firefly luciferase readouts were first normalized to their matching renilla luciferase readouts. Those readouts were then normalized to empty vector (pEM393 vector without any 3' UTR) controls and then the *let-7a* readouts (mimics and inhibitors) were normalized to their respective oligo controls.

Selection of *let-7* candidates. We selected 861 genes of interest based on computational prediction algorithms^{16,42–45}, experimental evidence, published literature, including known *let-7* target genes^{13,16,46–52} and mass spectrometry detectability¹⁴ (random controls). The predicted targets from the computational prediction algorithms were (i) from miRBase: based on the miRanda prediction algorithm version 3.0 (ref. 44) (*let-7* targets were downloaded on 25 April 2006; a *P*-value cutoff of 0.005 was applied); (ii) from Pictar: all *let-7* targets available at http://pictar.mdc-berlin.de/cgi-bin/new_PicTar_nematode.cgi?species=nematode downloaded 26 April 2006 (ref. 42); (iii) our 'Stark targets': *let-7* target prediction for *C. elegans* based on the algorithm described in reference 43 (A. Stark provided the target list); (iv) all the *let-7* targets published in reference 16; (v) all the *let-7* targets published in reference 45.

Design of SRM assays for *let-7*-related experiments. SRM assays were designed as previously described⁷ with minor adjustments. Briefly, proteotypic peptides (PTPs) were selected based on a large shotgun proteomics dataset¹⁴. This *C. elegans* proteome atlas dataset was filtered for a peptide-spectrum match false discovery rate of 0.17% corresponding to a protein identification false

discovery rate of 5% using Mayu¹⁵. Proteotypic peptides needed to contain at least one cysteine¹⁰, and doubly charged peptides with a high number of identifications were preferred. Four to eight fragment ions from the γ -ion series were computed for each peptide. Fragment ions (Q3) with a mass-to-charge ratio (m/z) above the peptide ion (Q1) and with a defined minimal distance to the peptide ion were chosen ($m/z_{Q3} - m/z_{Q1} \geq 50$ Thomson). The peptide ion/fragment ion (Q1/Q3) transitions were used to trigger the acquisition of MS2 spectra of the peptides of interest in *C. elegans* whole-worm extracts and in off-gel electrophoresis-fractionated samples (see below for SRM assay validation). Proteotypic peptides for additional 19 proteins not contained in the *C. elegans* proteome atlas were found using SRM-triggered MS2. For the samples derived from the off-gel electrophoresis fractionations, the isoelectric points of the peptides were predicted using BioPerl⁵³ and peptides were targeted in the predicted fraction and in the two neighboring fractions if available.

Database search and extraction of optimal SRM transitions for *let-7*-related experiments. The data were converted from the raw .wiff to the .mzXML format using the program mzWiff (version 3.5.3, build 16 April 2008 14:40:24). The MS2 spectra from the SRM-triggered MS2 experiments were searched against wormpep140 (<http://www.wormbase.org/>) using Sequest on a Sorcerer machine (3.10.4 release, SageN Research) with light ICAT as static modification and heavy ICAT and/or oxidized methionine as variable modifications. Precursor mass tolerance was set to 1.5 Da, and the data were searched fully tryptic (peptides with both ends corresponding to either N or C terminus of the corresponding protein or trypsin cleavage sites (after arginine or lysine not followed by proline) with maximal two missed cleavages. The data were filtered with a peptide-spectrum match FDR of 2.5% using PeptideProphet⁵⁴. Three transitions for each proteotypic peptide were generated by extracting the three highest fragment ions and the retention time of the peptide from the triple quadrupole MS2. All transitions used for quantification in this study are listed in **Supplementary Table 8**.

Mass spectrometry analysis of *let-7*-related experiments. The same instruments, a hybrid triple quadrupole-ion trap mass spectrometer (4000QTrap, ABI/MDS-Sciex) equipped with a nanoelectrospray ion source coupled to a Tempo nano LC system (Applied Biosystems) and settings were used as in reference 7. Briefly, for validations of SRM assays, the mass spectrometer was operated in SRM mode, triggering acquisition of a full MS2 spectrum upon detection of an SRM trace (MRM-triggered MS2, threshold 200 ion counts). The SRM transitions, generated as described above, were split and analyzed in several runs (an average of 60 transitions per run with a dwell time of 20 ms per transition). Each SRM acquisition was performed with Q1 and Q3 operated at unit resolution (0.7 m/z half-maximum peak width). MS2 spectra were acquired in enhanced product ion (EPI) mode for the two highest SRM transitions, using dynamic fill time, Q1 resolution low, scan speed 4000 amu s⁻¹, m/z range 300–1,400.

The complete transition list used for the quantifications is shown in **Supplementary Table 8**. An average of 60 transitions per run was used for the measurements. The quantification measurements were done in scheduled SRM mode (retention time window, 900 s and target scan time, 2 s).

Quantitative and statistical analysis of the let-7-related experiments. Peak height for the transitions associated to the *let-7(n2853)* (light ICAT label) and wild-type (heavy ICAT label) derived peptides were quantified using the software MultiQuant v. 1.1 Beta (Applied Biosystems). Log₂ fold changes (*let-7(n2853)*/wild type) were calculated for each transition separately. These values were then normalized using 11 proteotypic peptides (**Supplementary Figs. 1a and 4**) on each biological replicate separately. To test for statistically significant abundance changes, a two-sided, one-sample *t*-test was done on the normalized log₂ fold changes of the transitions grouped according to protein (mean of null hypothesis (μ) equal to zero). To generate our list of regulated candidates we used a $P \leq 0.01$ cutoff.

Sample preparation for miR-58-related experiments. WS4303 and WS5041 worms were always grown in parallel for each biological replicate at 25 °C. Four biological replicates of synchronized late L4 larvae were generated.

The protein samples were derived as has been described previously⁵⁵. We adapted the protocol accordingly. Briefly, after we collected the worms, we separated them from the bacteria by several washes in ice-cold buffer A (20 mM Tris-HCl (pH 8.0), 140 mM KCl, 1.8 mM MgCl₂, 0.1% Nonidet P-40 (NP-40) and 0.1 mg ml⁻¹ heparin), froze them in liquid nitrogen, and stored them at -80 °C until further use. One milliliter of frozen worm pellet was resuspended in 5 ml buffer B (buffer A plus 1.5 mM dithiothreitol (DTT), 1 mM phenylmethylsulfonyl fluoride, 0.5 µg ml⁻¹ leupeptin, 0.8 µg ml⁻¹ pepstatin, 20 U ml⁻¹ DNase I, 100 U ml⁻¹ RNaseOUT (Invitrogen) and 0.2 mg ml⁻¹ heparin). The resuspended worms were dropwise refrozen in liquid nitrogen and homogenized by a TissueLyser instrument (Qiagen) by four cycles of 4 min, each with a setting of 30 Hz; the metal containers with the samples were always refrozen in liquid nitrogen between the cycles. The purified worm extracts were incubated with 400 µl slurry (50% (v/v) IgG-agarose beads (Sigma) for 2 h at 4 °C. The supernatant representing the total extract was separated, and the beads were then used for the isolation of the TAP::ALG-1 containing complex. We used the supernatant for additional processing, as it was nearly identical to the total clarified lysates (only about 50% of the TAP::ALG-1 containing complex was missing).

Thereafter, the proteins were precipitated by acetone and resuspended in buffer (50 mM Tris-HCl (pH 8.3) and 8 M Urea) and the protein concentrations of the purified extracts were determined using the Bradford reagent (Sigma-Aldrich). The protein concentrations of the different extracts were adjusted to each other to minimize any bias for the further processing steps. Afterwards, 50 µg of total protein of each sample was mixed with 50 µg of total protein derived from ¹⁵N heavy isotope metabolically labeled adult worms (provided by R.F. Ketting and B.B. Tops)²⁵. The same metabolically labeled sample was mixed into all the 8 samples (four replicates of WS4303 and WS5041 worms). The metabolically labeled proteins were used as a normalization standard for all samples (for details, see below).

Finally, the tryptic digest and the following cation-exchange chromatography were performed as described previously³⁵. The peptide mixtures were cleaned by Sep-Pak tC18 cartridges (Waters) and eluted with 60% acetonitrile. All peptide samples were dried in a vacuum centrifuge, resolubilized in 2%

acetonitrile and 0.1% formic acid and frozen at -20 °C until they were analyzed on the mass spectrometer.

Design of SRM assays of miR-58-related experiments. We started with two protein lists of interest: 118 potential targets of miR-58 predicted with the TargetScan algorithm (http://www.targetscan.org/cgi-bin/targetscan/worm_12/targetscan.cgi?gid=&mir_c=miR-58&mir_nc=)^{20,21} and 44 randomly selected proteins as negative controls (from a set of 5,000 genes that are well expressed in L4 hermaphrodites, based on microarray data; unpublished data). We used the large *C. elegans* proteome atlas to determine peptides with good properties for mass spectrometric analysis¹⁴. For proteins with no or less than three PTPs available in the *C. elegans* proteome atlas, additional peptides with good MS properties were derived by bioinformatic prediction as previously²⁶, using the publicly available tool PeptideSieve⁹. PTPs had to be 7–18 amino acids long, must not have contained methionine or cysteine, had to be between 700–2,500 Da and had to map to one gene locus. To select the ‘best’ three PTPs, the priorities were number of charge 2 peptide-spectrum matches (descending), peptide length (ascending), peptide predicted isoelectric point (ascending) and PeptideSieve score (descending). Based on this filtering, we ordered peptides, synthesized them on a small scale in an unpurified format using the SPOT synthesis technology (JPT Peptide Technology), for 115 predicted targets (TargetScan) and 42 random control proteins. These peptides were prepared according to ref. 26 and were used to derive the optimal coordinates of the corresponding SRM assays (that is, best responding fragment ions, chromatographic elution time) by SRM-triggered MS2 (ref. 26). For each peptide (precursor charge 2 and 3) a transition corresponding to the first singly charged γ ion above the precursor m/z greater than ($m/z_{\text{precursor}} + 20$ Th) was generated and used as a trigger for a full MS2 spectrum.

Database search and extraction of optimal SRM transitions for miR-58 related experiments. Resulting raw MS2 .wiff data, generated by the SRM triggered MS2 runs, were converted to .mzXML format with the program mzWiff and searched against a database containing all the protein sequences of the targeted proteins (wormpep 140) using mascot (Version 2.1.0). A decoy database was generated by randomly reshuffling amino acids in between tryptic cleavage sites and appended to the target database. Precursor mass tolerance was set at 2 Da. The data were searched with full tryptic cleavage (maximally two missed cleavages) and filtered for a peptide-spectrum match FDR of 0.01 using Mayu¹⁵. For each peptide, the spectrum with the highest ion score was used to extract the five most intense fragment ions corresponding to the transitions used for quantification (doubly and triply charged). Fragments with m/z values close to the precursor ion m/z were discarded. Transitions corresponding to the metabolically heavy labeled proteins were calculated and added as well as decoy transitions that were used in the automated analysis of the data (**Supplementary Table 9**). The process was automated using in-house written Perl and R scripts (R Development Core Team. R: A Language and Environment for Statistical Computing).

Mass spectrometry analysis for miR-58-related experiments. The same instruments and settings as for the let-7-related experiments were used. Minor differences were that in the SRM

assays validation phase around 200 transitions (dwell time = 10 ms per transition) per run were targeted. Moreover, peptides that were not positively validated in the first set of runs were targeted again two more times.

The complete transition list used for quantifications is available in **Supplementary Table 9**. An average of 300 transitions per run was used for the measurements. The quantification measurements were done in the scheduled SRM mode (retention time window, 360 s and target scan time, 2.5 s).

SRM data processing for quantification of miR-58-related experiments. Raw SRM .wiff data were converted to .mzXML format with the program mzWiff. A peak detection algorithm was run on the data and several criteria of the signals were extracted to derive a score for the signal. Among the scores was a correlation score for expected relative intensities when compared to the relative intensities of the synthetic peptide measurement. Correlation of shape and coelution among light and of the light to the heavy transitions was also scored. A null model was derived from the measurement of negative controls (nonsense transitions or decoy transitions) included in the measurements. The scores were combined and a confidence score was calculated for the signals using the null model (L.R., O. Rinner, P.P., R. Hüttenhain, M. Beck, M. Brusniak *et al.*, unpublished data).

For quantification, the peak heights for one peptide were summed up. The summed peak heights were normalized using the signal of the isotopically heavy labeled peptide. After that, the \log_2 ratios of mutant to wild-type worms were calculated for each peptide measurement. For each protein, the average of this \log_2 ratio was calculated using the \log_2 ratios of all the peptides, charge states and biological replicates. A one sample Student's *t*-test (one-sided) was used to estimate a *P* value of regulation for the proteins.

31. Riddle, D.L., Blumenthal, T., Meyer, B.J. & Priess, J.R. *C. elegans II* (CSHL Press, 1997).
32. Miska, E.A. *et al.* Most *Caenorhabditis elegans* microRNAs are individually not essential for development or viability. *PLoS Genet.* **3**, e215 (2007).
33. Ding, L., Spencer, A., Morita, K. & Han, M. The developmental timing regulator AIN-1 interacts with miRISCs and may target the Argonaute protein ALG-1 to cytoplasmic P bodies in *C. elegans*. *Mol. Cell* **19**, 437–447 (2005).
34. Brenner, S. The genetics of *Caenorhabditis elegans*. *Genetics* **77**, 71–94 (1974).
35. Shiio, Y. & Aebersold, R. Quantitative proteome analysis using isotope-coded affinity tags and mass spectrometry. *Nat. Protoc.* **1**, 139–145 (2006).
36. Livak, K.J. & Schmittgen, T.D. Analysis of relative gene expression data using real-time quantitative PCR and the 2(-Delta Delta C(T)) Method. *Methods* **25**, 402–408 (2001).
37. Fraser, A.G. *et al.* Functional genomic analysis of *C. elegans* chromosome I by systematic RNA interference. *Nature* **408**, 325–330 (2000).
38. Kamath, R.S. *et al.* Systematic functional analysis of the *Caenorhabditis elegans* genome using RNAi. *Nature* **421**, 231–237 (2003).
39. Timmons, L. & Fire, A. Specific interference by ingested dsRNA. *Nature* **395**, 854 (1998).
40. Rual, J.F. *et al.* Toward improving *Caenorhabditis elegans* phenome mapping with an ORFeome-based RNAi library. *Genome Res.* **14**, 2162–2168 (2004).
41. Mangone, M., Macmenamin, P., Zegar, C., Piano, F. & Gunsalus, K.C. UTRome.org: a platform for 3'UTR biology in *C. elegans*. *Nucleic Acids Res.* **36**, D57–D62 (2008).
42. Lall, S. *et al.* A genome-wide map of conserved microRNA targets in *C. elegans*. *Curr. Biol.* **16**, 460–471 (2006).
43. Stark, A., Brennecke, J., Bushati, N., Russell, R. & Cohen, S. Animal microRNAs confer robustness to gene expression and have a significant impact on 3' UTR evolution. *Cell* **123**, 1133–1146 (2005).
44. Griffiths-Jones, S., Saini, H.K., Dongen, S.V. & Enright, A.J. miRBase: tools for microRNA genomics. *Nucleic Acids Res.* **36**, D154–D158 (2008).
45. Watanabe, Y. *et al.* Computational analysis of microRNA targets in *Caenorhabditis elegans*. *Gene* **365**, 2–10 (2006).
46. Johnson, S.M. *et al.* RAS is regulated by the let-7 microRNA family. *Cell* **120**, 635–647 (2005).
47. Ding, X.C., Slack, F.J. & Grosshans, H. The let-7 microRNA interfaces extensively with the translation machinery to regulate cell differentiation. *Cell Cycle* **7**, 3083–3090 (2008).
48. Abrahamte, J.E. *et al.* The *Caenorhabditis elegans* hunchback-like gene lin-57/hbl-1 controls developmental time and is regulated by microRNAs. *Dev. Cell* **4**, 625–637 (2003).
49. Slack, F.J. *et al.* The lin-41 RBCC gene acts in the *C. elegans* heterochronic pathway between the let-7 regulatory RNA and the LIN-29 transcription factor. *Mol. Cell* **5**, 659–669 (2000).
50. Lin, S.Y. *et al.* The *C. elegans* hunchback homolog, hbl-1, controls temporal patterning and is a probable microRNA target. *Dev. Cell* **4**, 639–650 (2003).
51. Papadopoulos, G.L., Reczko, M., Simossis, V.A., Sethupathy, P. & Hatzigeorgiou, A.G. The database of experimentally supported targets: a functional update of TarBase. *Nucleic Acids Res.* **37**, D155–D158 (2009).
52. Xiao, F. *et al.* miRecords: an integrated resource for microRNA-target interactions. *Nucleic Acids Res.* **37**, D105–D110 (2009).
53. Stajich, J.E. *et al.* The Bioperl toolkit: Perl modules for the life sciences. *Genome Res.* **12**, 1611–1618 (2002).
54. Keller, A., Eng, J., Zhang, N., Li, X. & Aebersold, R. A uniform proteomics MS/MS analysis platform utilizing open XML file formats. *Mol. Syst. Biol.* **1**, 2005.0017 (2005).
55. Gerber, A.P., Herschlag, D. & Brown, P.O. Extensive association of functionally and cytotopically related mRNAs with Puf family RNA-binding proteins in yeast. *PLoS Biol.* **2**, E79 (2004).

Erratum: A quantitative targeted proteomics approach to validate predicted microRNA targets in *C. elegans*

Marko Jovanovic, Lukas Reiter, Paola Picotti, Vinzenz Lange, Erica Bogan, Benjamin A Hirschler, Cherie Blenkiron, Nicolas J Lehrbach, Xavier C Ding, Manuel Weiss, Sabine P Schrimpf, Eric A Miska, Helge Großhans, Ruedi Aebersold & Michael O Hengartner
Nat. Methods 7, 837-842 (2010); published online 12 September 2010; corrected after print 9 November 2010

In the version of this article initially published, the reported *P* values were incorrectly written and an incorrect wording change was inadvertently made to the Figure 1 legend. The errors have been corrected in the HTML and PDF versions of the article.